ARCHIVES OF METALLURGY AND MATERIALS
Volume 51 2006 Issue 1

G. MRÓWKA-NOWOTNIK*, J. SIENIAWSKI*, A. NOWOTNIK*

INFLUENCE OF PRECIPITATION STRENGTHENING PROCESS ON THE MECHANICAL PROPERTIES OF 6082 WROUGHT ALUMINIUM ALLOY

WPŁYW PROCESU UMACNIANIA WYDZIELENIOWEGO NA WŁAŚCIWOŚCI MECHANICZNE STOPU ALUMINIUM DO PRZERÓBKI PLASTYCZNEJ 6082

Aluminium alloys containing Mg and Si as the major solutes are strengthened by precipitation of the metastable precursors of the equilibrium β (Mg_2Si) phase in one or more sequences. There are several particles that can form during aging: GP zones and intermediate metastable phases -β", β' and stable β phase [1-10]. Although the precipitation process in Al-Mg-Si alloys has been extensively studied, the understanding of the hardening process is still incomplete, since any change in composition, processing and aging practices could affect the precipitation hardening behaviour [3-6, 10]. In this paper differential scanning calorimetry (DSC), transmission electron microscopy (TEM), and hardness measurements have been utilized to study the effect of the precipitation hardening on the mechanical properties in aluminium alloy 6082. The mechanical (R_m and $R_{p0.2}$) and plastic (A) properties of the alloy were evaluated by uniaxial tensile tests at room temperature. The results show that the microstructure and mechanical properties change during artificial aging due to the precipitation strengthening process. Therefore, the parameters (time and aging temperature) of precipitation strengthening process that may lead to the most favourable mechanical properties of 6082 alloy were determined.

Keywords: precipitation strengthening, mechanical properties, hardness, 6082 alloy, DSC

Umacnianie stopów AlMgSi następuje wskutek wydzielania się metastabilnych faz przejściowych prowadzących do utworzenia się stabilnej równowagowej fazy β (Mg_2Si) Wydzielanie metastabilnych faz przejściowych jest dość złożone i nie do końca poznane. Najczęściej spotykany w literaturze schemat procesu rozpadu przesyconego roztworu stałego w umacnianych wydzieleniowo stopach AlMgSi ma postać: $\alpha \rightarrow$ GP$\rightarrow \beta$"$\rightarrow \beta$'$\rightarrow \beta$(Mg_2Si) (α – przesycony roztwór stały, GP – strefy Guinier'a-Prestona, β" i β' – metastabilne fazy przejściowe, β – faza stabilna, równowagowa). Mimo, że procesy wydzielania w stopach AlMgSi były przedmiotem wielu badań, temat ten jest wciąż aktualny. Zmiana np.: składu chemicznego stopów, czy warunków procesu starzenia, wpływa na procesy umocnienia. W artykule zastosowano badania kalorymetryczne, mikroskopię elektronową oraz badania twardości w celu zbadania wpływu czasu i temperatury starzenia na mikrostrukturę oraz właściwości mechaniczne stopu aluminium 6082.

1. Material and experimental

An alloy 6082 containing 0.78 Mg, 1.2 Si, 0.33 Fe, 0.08 Cu, 0.5 Mn, 0.05 Zn and 0.14 Cr (wt.%) was cast in SAPA Aluminium-Trzcianka company. A 50 kg ingot was homogenized at 500°C, and then extruded into a extrudate profile of rectangular cross section (40×100 mm). The test specimens were cut from the ingot parallel to the extrusion direction. To get different microstructures, the following heat treatments were performed: the alloy was solution-treated at 570°C for 4 h, followed by a water quench; then the specimens were aged at 130, 190 and 220°C for 72, 42 and 48 h, respectively. The specimens were strained by tensile deformation on an Instron-type machine at room temperature. The hardness was measured with Brinell tester under 49.03 N load for 10 sec. TEM observations were conducted on a transmission electron microscope (Jeol JEM 2010 ARP) operated at 200 kV. The foils were prepared by twin-jet electropolishing in a solution CH_3OH + $HClO_4$ + glycerine, operating at -10°C and U = 28 V. DSC samples were investigated in SETARAM Setsys thermal analyzer fitted with a scanning difrerential calorimeter module, under Ar atmosphere. The heat effects associated with precipitation of GP zones and inter-

* RZESZÓW UNIVERSITY OF TECHNOLOGY, DEPARTMENT OF MATERIALS SCIENCE, 35-959 RZESZÓW, 2 W. POLA ST., POLAND

mediate metastable phases were obtained by substracting a baseline obtained with super pure Al run.

2. Results and discussion

Fig. 1 shows thermogram of the 6082 alloy obtained at a heating rate of 10°C/min immediately after quenching from the solutionizing temperature. The DSC scan reveals that six exotermic events occur during heating from room temperature to 630°C. The peaks can be observed at following temperatures: **I**-83, **II**-164, **III**-260, **IV**-311, **V**-475 and **VI**-533°C. With respect to the literature [4, 5, 9], the precipitation sequence during heating the aluminium alloy 6082 is as follows: α (sss)→ GP zones → β" → β' → β; where α (sss) is the supersaturated solid solution, GP – Guinier-Prestone zones, β", β' – intermediate metastable phases. DSC results and TEM observation (Fig. 4, 5) are quite similar to those observed previously by B r o i l i [9] and M i a o [7] and confirm above mentioned precipitation sequence. As can be observed in Fig. 1, for 6082 alloy the first two exothermic peaks (I and II) correspond to the beginning of precipitation of GP zones while the others correspond to precipitation of metastable phases. Judging from the position of these peaks, the main precipitates in 260°C and 310°C aged alloys are metastable β" and metastable β', respectively. The peak at the higher temperature is the strongest one (III-250°C) and corresponds to the precipitation of intermediate metastable β" phase. These results are quite consistent with recent analysas (e.g. M i a o [7] and [4-6, 9]).

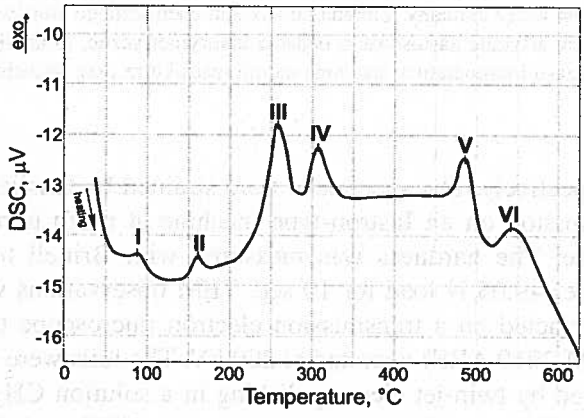

Fig. 1. DSC trace of an as-quenched sample taken at a scan rate of 10°C/min

Fig. 2 shows the effect of artificial aging time on hardness. It can be seen that the hardness of 6082 alloy effectively depends on the precipitation strenghtening conditions. The graphs indicate that, in all the cases except at an aging at 130°C, the hardness initially increases rapidly with the increase in aging time reaching the peak value, after which hardness almost returns toward its initial value. The alloy reached a maximum hardness value of 127 HB after 4 hours of aging at 190°C. Similar hardness value to that observed for the highest aging temperature the alloy achieved at aging temperature of 130°C although after longer aging time – 70 h. It was affirmed that the higher aging temperature, the shorter time is needed to achieve the maximum hardness value. The observed changes in hardness in artificial aging may be essentially attributed to the precipitation process of $\beta(Mg_2Si)$ particles. The results obtained and results reported previously [4-7] have enabled to conclude that the aging process for 6082 alloy at 130°C begins with the formation of GP zones which act as obstacles to dislocation motion and results in slight hardness increase. At the higher aging time, the GP zones are replaced initially by precipitation of metastable intermediate β" and finally by precipitates of β' phases, hence more hardening and an accelerated rate of aging process is noted. The hardness of the alloy increase as far as the equilibrium stable $\beta(Mg_2Si)$ phases is formed. Observed a drop in hardness at prolonged aging times at 190 and 220°C could be attributed to the effect of the overaging of the alloy. Extended aging time and elevated temperature contribute to the formation of larger plate-shaped precipitates. TEM examination of microstructures in the samples after aging at 130 and 220°C confirms changes in precipitates size (Fig. 4).

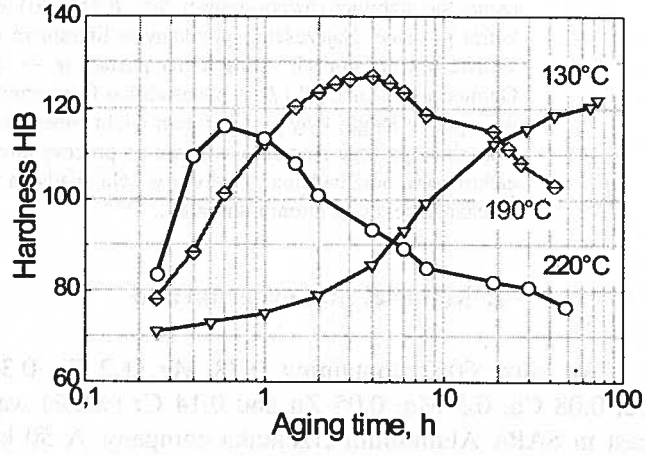

Fig. 2. Variation of hardness with time during artificial aging

GP zones formation stage does not occur during aging at 190°C. In this case, the aging process starts with the precipitation of intermediate phases – β" and β'. Thus the hardness peaks at aging curves appears after shorter time (at 190°C after 5 hours) that correlates with the presence in the microstructure of partially coherent non-equilibirum precipites of β" and β' phases. Application of higher aging temperature – 220°C results in

reduction of time which is required for achieving the maximum hardness value. The alloy achieves its maximum hardness at 220°C when aged for 1 h, thereafter, a decrease occurs as the time progresses. The drop in hardness observed in the aging curve obtained for aging at the highest temperature – 220°C could be due to formation of equilibrium phase of $\beta(Mg_2S)$ followed by its growth to larger particles size (Fig. 4). Further heat treatment at higher temperature and time may result in coalescence of $\beta(Mg_2S)$ phase precipitates. Fig. 3 shows a bright field TEM image representing the typical microstructure of the material solutionized and aged for 6 h at 160°C. The image shows small needle shaped β" particles aligned in {001} matrix direction and homogeneously distributed throughout the matrix. The presence of a large number of tiny dots represents the β" needles viewed end-on. This indicates that β" is the main strengthening phase in 6082 alloys. The microstructure is quite similar to that reported by Gupta [4] and Miao [7] on an 6022 alloy.

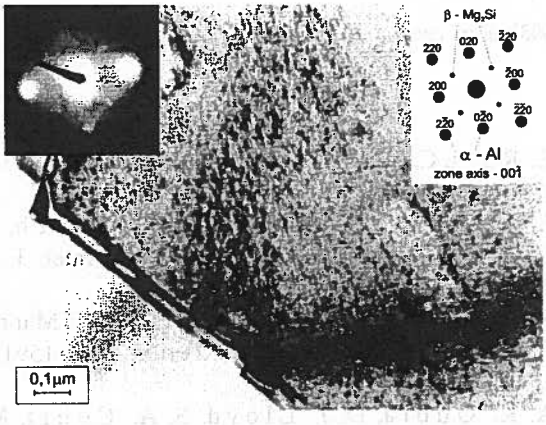

Fig. 3. TEM micrograph of 6082 alloy aged at 160°C for 6 h showing uniform dispersion of fine needle shaped β" particles

Fig. 4 shows the typical microstructure of the alloy aged for 20 h at 300°C. Upon prolonged aging, the β" needles are similar to those observed in Fig. 3, except they are larger. The β" needles occupy, in a homogeneous way, the whole volume of the grains. As shown in Fig. 4 the microstructure also contained non- uniform dispersion of intermetallic particles which were most commonly spherical in shape. These large particles were analysed using a STEM and all of them were found to contain Al, Fe, Mn and Si suggesting that they were precipitates of α-Al(FeMn)Si phase.

The tensile ($R_{p0.2}, R_m$) and plastic properties (A) of the alloy aged at 130°C are shown in Fig. 5. It should be noted that the yield strength and tensile strength of the alloy increase with increasing aging time with almost no ductility changes. The yield strength increases continuously with time. A significant increase in mechanical properties was achieved during aging for up to 20 h. Further heating causes a steady increase in the yield strength of the material. The increment of alloy strength similarly to the observed increment in hardness can be treated as the effects of initial formation of GP zones followed by precipitation of metastable particles of β" and β' phases. Relatively high values of correlation coefficient (see equation in Fig. 5b) provide evidence that mechanical properties strongly depend on aging time at this temperatures.

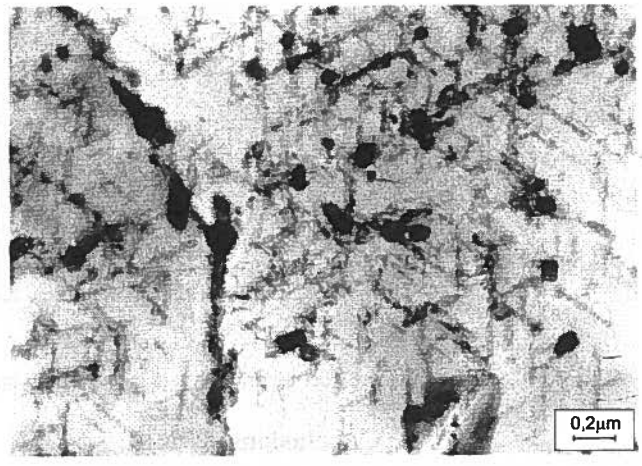

Fig. 4. A bright-field image of 6082 alloy aged at 300°C for 20 h showing coarser needle-like β" particles on dislocations as well as globular precipitates of α-Al(FeMn)Si phase

The curves of $R_m, R_{p0.2}$ and A obtained at aging at 190°C are shown in Fig. 6. These results confirm those obtained earlier. After heat treatment for the first few hours yield strength and tensile strength increases rapidly. The growing trend of strength continues and it reaches R_m = 440 MPa after aging for 6 hours. Further extension of aging time results in insignificant variations of R_m and $R_{p0.2}$ values (Fig. 6a). The reason for this is the same as in the case of aging at lower temperature mentioned above. However in case of higher temperature of aging – 190°C the maximum of the strength properties is achieved after shorter time of exposing the alloy to an elevated temperature.

Fig. 6b represents the curves obtained in tensile static tests for the alloy artificially aged at the highest temperature of 220°C. There is a roughly linear drop of both yield strength and tensile strength with aging time. For exemple, the yield strength decreases significantly from its maximum 395 MPa to a value of less than 300 MPa after 30 h of aging. The maximum $R_{p0.2}$ value was recorded after 1 h of aging. However, the plastic properties increase with increasing time. Initially a small deterioration of elongation value was observed but at higher aging times up 5 hours the elongation values increase steadily.

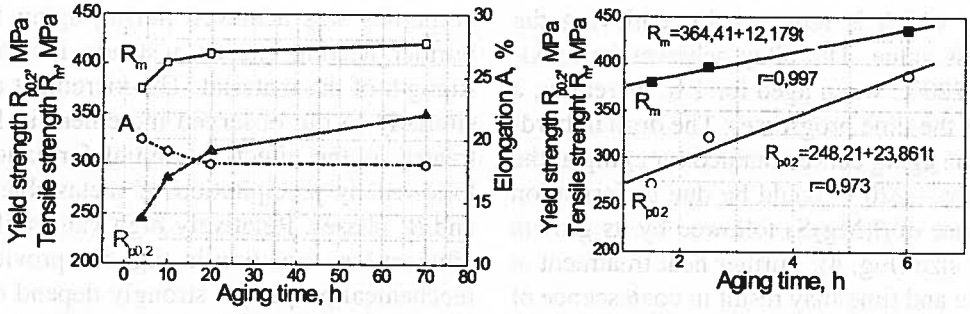

Fig. 5. Effect of time on tensile and yield strength of 6082 Al-alloy aged at 130°C

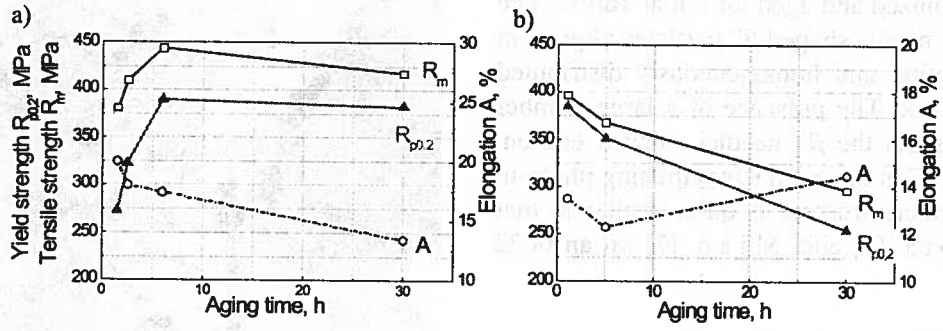

Fig. 6. Effect of time on tensile and yield strength of 6082 alloy aged at: a) 190 and b) 220°

3. Conclusions

The aging kinetics of 6082 Al-alloy was studied after aging at three different temperatures and for various times. The experimental results show that the highest hardness and mechanical properties (yield strength and tensile strength) were obtained after aging at 190°C for 6 hours. In addition the plastic properties of the alloy aged at this temperature are much greater than the value obtained in the case of aging at 220°C. The initial increase in the hardness and strength properties, is due to initial precipitation of GP zones and then formation of very fine needle-shaped particles of metastable phases – β" and β' in under-aged and peak-aged conditions. These precipitates effectively interfere with the motion of dislocations. A decrease in the hardness and mechanical properties of the alloy in the over-aged conditions (increase in aging time and temperature) has occurred because of coalescence of the precipitates into larger particles of metastable β" and β' phases.

Acknowledgements

This work was carried out with the financial support of the Polish State Committee for Scientific Researches under grant No. 3T08B 078 27 and U-6572/BW.

Received: 5 January 2006.

REFERENCES

[1] C. Ravi, C. Wolverton, Acta Mater. **52**, 4213-4227 (2004).
[2] J. J. Gracio, F. Barlat, E. F. Rauch, P. T. Jones, V. F. Neto, A. B. Lopes, Inter. J. Plast. **20**, 427-445 (2004).
[3] R. G. Kamat, J. F. Butler, S. J. Murtha, F. S. Bovard, Mater. Sci. Forum **396**, 1591-1596 (2002).
[4] A. K. Gupta, D. J. Lloyd, S. A. Court, Mater. Sci. Eng. **A316**, 11-17 (2001).
[5] A. K. Gupta, D. J. Lloyd, S. A. Court, Mater. Sci. Eng. **A301**, 140-146 (2001).
[6] G. A. Edwards, K. Stiller, G. L. Dunlop, M. J. Couper, Acta Mater. **46**, 11, 3893-3904 (1998).
[7] W. F. Miao, D. E. Laughlin, Scripta Mater. **40**, 7, 873-878 (1999).
[8] L. Zhen, S. B. Kang, Mater. Let. **37**, 349-353 (1998).
[9] G. Biroli, G. Caglioti, L. Martini, G. Riontino, Scripta Mater. **39**, 2, 197-203 (1998).
[10] M. Murayama, K. Hono, M. Saga, M. Kikuchi, Mater. Sci. Eng. **A250**, 127-132 (1998).